PCCP

Accepted Manuscript

Challenging Compounds for Calculating Molecular Second Hyperpolarizabilities: the Triplet State of the Trimethylenemethane Diradical and Two Derivatives

Marc de Wergifosse,[1] Benoît Champagne,[1] Soichi Ito,[2] Kotaro Fukuda,[2] and Masayoshi Nakano[2]

[1] *University of Namur, Laboratory of Theoretical Chemistry, Rue de Bruxelles 61, 5000 Namur – Belgium*

[2] *Department of Materials Engineering Science, Graduate School of Engineering Science, Osaka University, Toyonaka, Osaka 560-8531 (Japan)*

ABSTRACT

The second hyperpolarizability γ of trimethylenemethane (TMM) and two 1,3-dipole derivatives (NXA and OXA) in their triplet ground state has been evaluated at the UCCSD(T) with the d-aug-cc-pVDZ extended basis set, highlighting that γ decreases from TMM to NXA and OXA, following the opposite order of their permanent dipole moments. These results are then used to benchmark a broad range of levels of approximation. So, the UMP2, UMP4, and UCCSD methods can be used to characterize γ of TMM and NXA but not of OXA. In that case, the large field-induced charge transfer contribution is difficult to handle by the MPn methods and only the UCCSD method provides values close to the UCCSD(T) reference. Turning to the performance of DFT with typical exchange-correlation functionals, the UM06-2X functional, which contains 54% of HF exchange, performs very well with a maximum of 4.5% of difference with respect to the reference values. On the other hand, employing less HF exchange leads to an overestimation of the responses whereas range-separated hybrids generally underestimate the second hyperpolarizabilities. Finally, the use of spin-projected methods for these 1,3-dipole triplet molecules has a little impact since the spin contamination is almost negligible.

1

I. INTRODUCTION

Electron correlation plays a central role in the prediction of the molecular second hyperpolarizabilities (γ) of closed-shell and open-shell systems.[1-11] Two major types of methods are currently employed to evaluate accurately the molecular γ responses: wave function methods[12-24] and density functional theory (DFT) approaches[25-34]. Due to their computational requirements, wave function methods can only be applied to small (or medium-sized) systems. Nevertheless, they can be used as references in order to assess the reliability of DFT worked out with different approximate exchange-correlation (XC) functionals. Still, the methods requirements are different for small and large systems. Indeed, in the case of small molecules, an accurate description of the most delocalizable and outermost part of the electron distribution is needed as well as of their hyperpolarization effects.[20,25,35] On the other hand, for large systems like oligomer chains or push-pull π-conjugated chromophores, for example, most of the response is attributed to the hyperpolarization of the molecular (monomer) units and to charge transfer effects.[36,37] There, a proper treatment of the intramolecular long-range delocalization is needed.

The second hyperpolarizability of small compounds has fascinated the scientific community since a long time. For example, in 1995, Nakano *et. al.*[38] have studied the static second hyperpolarizabilities of open-shell systems and in particular their dependence on the basis set and electron correlation effects. It was found that the MP2 method with an extended (split-valence + polarization) basis set including diffuse p and d functions gives a reasonable description of relative tendencies of γ for H_2NO (nitroxide radical), H_2CO (formaldehyde) and, $(CH_3)_2CO$ (acetone), while the use of the CCSD(T) method is crucial for the qualitative description of γ of $(CH_3)_2NO$. Later on, using the same methods, Yamada *et. al.*[35] have investigated the spatial distribution of the third-order electric field derivatives of the electron density ($d^\gamma(\vec{r})$, called the γ density[39]) of H_2NO and H_2CO. They concluded that the correct spatial characteristics of the $d^\gamma_{zzz}(\vec{r})$ contour plots of H_2NO cannot be reproduced at the MP2 level in contrast to those of H_2CO. The same year, Maroulis[40] has reported an extensive study on carbon monoxide. He described the bond length dependence of the second hyperpolarizability at the CCSD(T) level of theory, which leads to a very good agreement with experimental electric field-induced second harmonic generation γ values. In 1998, Maroulis and Pouchan[41] have investigated the linear and nonlinear polarizability of two triply-bonded linear molecules: HCN and HCP. They found that electron correlation modifies mainly the longitudinal component of γ. For HCN, the mean CCSD(T) γ value is 17.4% larger than the HF one. In the case of HCP, the CCSD(T) value is only 2.2% larger. In 1999, Yamada *et. al.*[42] elucidated the

second hyperpolarizabilities for n-center radical systems (n, integer) i.e., one-center BH_3^-, CH_3, and NH_3^+, and three-center $BH(CH_2)_2^-$, $CH(CH_2)_2$, and $NH(CH_2)_2^+$ radical models by employing various electron-correlation and a density functional methods using extended basis sets. They showed that the one-center radicals exhibit positive γ values at high-order electron correlation level using sufficiently large basis sets, while, for the three-center radicals, only $NH(CH_2)_2^+$ is found to possess negative γ. Xenides and Maroulis[43] have reported accurate values for the static first and second hyperpolarizabilities of SO_2, in 2000. Those have been obtained at the CCSD(T) level of theory with a basis set rich in d-gaussian type functions on both sulfur and oxygen. In the year 2004, Nakano *et. al.*[44] have investigated the spin multiplicity effects (doublet, quartet, and sextet states) on the second hyperpolarizability for a smal-sized open-shell neutral conjugated model, the C_5H_7 radical. They have shown that γ increases with the spin multiplicity, suggesting the interest for designing such spin-enhanced nonlinear optical systems. In 2010, Maroulis and Menadakis[45] used very large purpose-oriented Gaussian-type basis sets to determine static electric (hyper)polarizabilities of nitrous oxide and carbonyl sulphide. The best values they have reported are obtained at the CCSD(T)/[9s6p4d2f/9s6p4d2f/9s8p4d2f] level of theory for carbonyl sulphide and at the CCSD(T)/[9s6p4d1f/ 9s6p4d1f/9s6p4d1f] for nitrous oxide. These studies point out that the amplitude of the electron correlation effects on γ (as well as on β, the first hyperpolarizability) depends much on the molecular nature that highly correlated methods (UCCSD, UCCSD(T), and UQCISD) are often necessary for quantitative or semi-quantitative descriptions.

In this article, we consider 1,3-dipole diradical molecules and in particular trimethylenemethane (TMM), which was first isolated by Dowd in 1966.[46] It was found that the ground state of this diradical compound has a pure triplet multiplicity. Indeed, in 1976, Dowd and coworkers showed that TMM exhibits a triplet state electron paramagnetic resonance (EPR) spectrum.[47] After that, Dowd has also attempted to determine its singlet-triplet splitting of 7 kcal/mol.[48,49] This was finally measured by photoelectron spectroscopy in 1996.[50] With its fascinating electronic structure, TMM has attracted the attention of the theoretical chemistry community since a long time.[51-82] In 1977 Borden and Davidson explored by *ab initio* calculations, employing an STO-3G basis set and including the full π-space CI, the potential energy surface of its two lowest singlet states.[57] In 1974, Yarkony and Schaefer characterized for the first time the triplet electronic ground state of TMM.[53] This article was followed by a plethora of studies on the determination of the TMM singlet-triplet splittings.[53-55,60-62,64,66-69,71,73-76] More recently in 2003, Slipchenko and Krylov characterized the electronic structure of TMM diradical in its triplet ground

and spin-flip electronically excited states.[78] Their study was an opportunity to demonstrate that the spin-flip method is a reliable tool for studying diradicals.

In the present work, the second hyperpolarizability of the triplet state of 1,3-dipole models (R-X-R where R = CH_2, and X = $C=CH_2$, $C=O$, or $C=NH$), including TMM (R = CH_2), is investigated. Like in our previous study on *p*-quinodimethane derivatives[10], wave function- and DFT-based results are compared to benchmark values evaluated with the unrestricted coupled cluster method including single and double excitations as well as a perturbative estimate of the triples [UCCSD(T)]. Indeed, the UCCSD(T) method has previously been shown to provide, for the multiradical H_4 model compound, γ values in close agreement with Full CI results.[83] In parallel, the basis set effects are investigated as well as the use of spin-projected UMPn methods, which was also used by some of us in 2005 on model π-conjugated compounds.[84]

II. THEORETICAL AND COMPUTATIONAL APPROACHES

The geometrical parameters of the three molecules as well as their molecular orientations are given in figure 1.[85] The γ values were calculated using the finite field approach combined with the automatic Romberg differentiation procedure.[86] In all the FF computations, a geometrical progression of field amplitudes was used: $\pm 2^k$ 0.0002 or $\pm 2^k$ 0.0004 with k going, respectively, from 0 to 6 or from 0 to 5. Tight convergence criteria on the energies were used from 10^{-9} to 10^{-11}. All the γ values have been computed with unrestricted methods. This includes the Hartree-Fock (HF) method, the Møller-Plesset perturbation theory approach truncated to second (MP2), third (MP3), and fourth (MP4) orders as well as (SDQ-MP4), the coupled cluster approach including all single and double excitations with [CCSD(T)] and without (CCSD) a perturbative estimate of the triples. A range of basis sets was employed: aug-cc-pVDZ, aug-cc-pVTZ, and d-aug-cc-pVDZ basis sets (the number of basis functions for the three compounds are given in table S1. These are standard basis sets, directly available from the Gaussian package[87]. The *s*-fold spin-projection scheme was also employed.[88] It consists in removing the successive spin contamination contributions from the UHF and UMPn energies. At the UHF level, up to *s*=6 spin projections (*P*-) were carried out exactly whereas at the UMPn (n = 2-4) levels they were done limited to *s*=4. No spin-projection method was used for the coupled cluster energies since these methods are known to suffer less from spin contamination. Electron core correlation was considered in the calculations, which amounts to an impact of a few percents on the γ values. For instance, for TMM, UCCSD(T)/aug-cc-pVDZ level calculations give γ values of 16658 a.u. and 15997 a.u. (-4%) with and without core correlation, respectively.
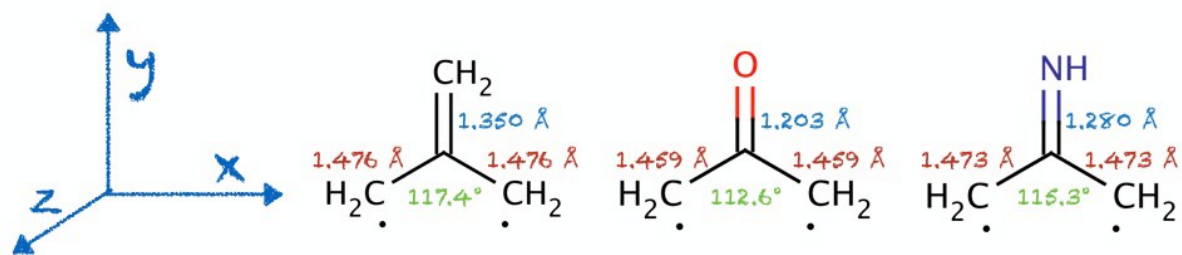
Figure 1. Structures, geometrical parameters, and molecular orientations of the three 1,3-dipole compounds.

Unrestricted DFT computations with several XC functionals were performed to assess the effect of the functional and particularly the role of HF exchange: i) the BLYP generalized gradient-approximation functional, ii) the B3LYP and BHandHLYP hybrids, iii) the LC-BLYP ($\mu = 0.33$) and LC-BLYP ($\mu = 0.47$) range-separated hybrids, and iv) the M06 and M06-2X meta-generalized gradient-approximation functionals. BLYP, B3LYP, BHandHLYP, and M06-2X XC functionals include 0%, 20%, 50%, and 54% of HF exchange, respectively. LC-BLYP is a long-range-separated functional, which contain 100% of HF exchange at large inter-electronic distances. The Ewald partitioning is used in this functional in order that the electron-electron repulsion operator is partitioned in a short-range part described by non-local DFT functionals and a long-range part where the exchange is described by HF exchange. The range-separating parameter μ dictates the transition between short- and long-range. For LC-BLYP, two range-separated parameters were used, the original one ($\mu = 0.33$) and the default ($\mu = 0.47$) in Gaussian 09. Their choices are substantiated by a study due to Bonness *et. al.*[89] showing that the LC-UBLYP method with $\mu = 0.3$–0.5 is adequate for calculating γ of π-conjugated diradical systems while it does not suffer from the catastrophic behavior found in conventional exchange–correlation functionals.

Since spin-projection turns out to be important to reproduce UCCSD(T) benchmark values, we have incorporated results obtained with the approximate spin-projection DFT scheme proposed by Nakano and coworkers[90] in combination with the automatic Romberg differentiation procedure[86] we have developed last year. Approximate spin-projected DFT γ values were then computed from the field dependence of the spin-projected electron density. Indeed, when using an unrestricted method, in order to remove the spin contamination, the electron density can be replaced by the spin-projected-corrected density.[90] By applying the perfect-pairing spin-projection scheme to the occupation numbers n_k obtained from spin-unrestricted single-determinant methods, the spin-projected occupation numbers n_k^{SP} read:

$$n_{HONO-i}^{SP} = \frac{\left(n_{HONO-i}\right)^2}{1 + \left(\dfrac{n_{HONO-i} - n_{LUNO+i}}{2}\right)^2}$$

$$n_{LUNO+i}^{SP} = \frac{\left(n_{LUNO+i}\right)^2}{1 + \left(\dfrac{n_{HONO-i} - n_{LUNO+i}}{2}\right)^2}$$
(1)

Then, the approximate spin-projected one-electron density $d^{SP}(\vec{r})$ is expressed as:

$$d^{SP}(\vec{r}) = \sum_{i=0}^{N/2-1} \left[n_{HONO-i}^{SP} \phi_{HONO-i}^*(\vec{r}) \phi_{HONO-i}(\vec{r}) + n_{LUNO+i}^{SP} \phi_{LUNO+i}^*(\vec{r}) \phi_{LUNO+i}(\vec{r}) \right].$$
(2)

The differentiation procedure consists in combining spin-projected-corrected electron density tensor grids obtained for a succession of k external electric fields, of which the amplitudes form a geometrical progression. The spin-projected static γ tensor components can then be obtained by applying the automatic Romberg differentiation procedure[86] where the zero-order iteration γ tensor values are obtained by the integration of the position vector over the γ density tensor component grid:

$$\gamma_{mijl}(k,0) = -\int_{grid} r_m \, d_{ijl}^\gamma(\vec{r}, k) d\vec{r} \ .$$
(3)

The geometrical progression of field amplitudes employed here uses the same parameters as in other, energy-based, FF calculations. In those computations, particular attention has been paid to the grid parameters and to the accuracy of the numerical integration. Cubes were generated every 0.1 Å in a parallelepiped box with ± 4 Å of void around the molecule.

The γ_{xxxx}, γ_{yyyy}, γ_{zzzz}, γ_{xxyy}, γ_{xxzz}, and γ_{yyzz} components of the γ tensor have been computed as well as the mean of γ, which reads:

$$\gamma_{mean} = \frac{\gamma_{xxxx} + \gamma_{yyyy} + \gamma_{zzzz} + 2\left(\gamma_{xxyy} + \gamma_{xxzz} + \gamma_{yyzz}\right)}{5}.$$
(4)

The T convention was used for the definition of γ. All the calculations were performed with the Gaussian 09 package.[87] The T-REX program was used for the automatic Romberg differentiation procedure.[86]

III. RESULTS AND DISCUSSIONS

III.a. WAVE FUNCTION METHODS

The γ_{mean} of TMM, OXA, and NXA molecules, evaluated at the UHF, UMPn, and UCC level of theory with the selected basis sets, are presented in figures 2, 3, and 4, respectively. These figures

also include *s*-fold spin-projected UHF, and UMPn values. Table 1 summarizes the γ_{mean} values obtained with the d-aug-cc-pVDZ basis set. Corresponding data for the γ_{xxxx}, γ_{yyyy}, and γ_{zzzz} components are provided in Supporting Information (Figures S1, S2, and S3).

For the TMM molecule, UMP2, UMP4, and UCCSD methods provide a good estimate of the γ_{mean} UCCSD(T) reference value, with only 6.7%, 8.5%, and 8.9% of underestimation, respectively. Since the spin contamination is very small, the projected schemes do not make any improvements. In fact, only the first-order spin-projection correction is not negligible and leads to a decrease of γ_{mean} by less than 10% at the UMPn levels of approximation. By looking at the different γ tensor components (Figure S1), it appears that electron correlation effects are very similar for all diagonal components, as well as for the three selected basis sets. Only a small increase of the response is observed between aug-cc-pVDZ and aug-cc-pVTZ basis sets. This amount is between 5.8% (SDQ-UMP4) and 8.0% (UMP2) for the γ_{xxxx} component. Using the d-aug-cc-pVDZ basis set leads to similar but shifted UMP2, UMP4 and UCCSD values with a difference maximum of 2.4%. This is not observed for the UCCSD and UCCSD(T) methods where going from aug-cc-pVDZ to the d-aug-cc-pVDZ has a larger effect, *i.e.* an increase of γ_{xxxx} by 20.5% and 27.0% at the UCCSD and UCCSD(T) levels, respectively. Basis set effects get however much smaller when going from the d-aug-cc-pVDZ to the d-aug-cc-pVTZ basis sets. Indeed, the UHF and UMP2 γ_{mean} values with the d-aug-cc-pVTZ basis set amount to 122 10^2 a.u. and 205 10^2 a.u., respectively. This supports the use of the d-aug-cc-pVDZ basis set rather than the aug-cc-pVTZ though they have similar numbers of basis functions. A similar choice was also done previously for calculating the β of small reference molecules.[20,24]

In the case of γ_{mean} of OXA, at first look, electron correlation effects are quite dissimilar to those of TMM. The closest value to UCCSD(T) is obtained at the UCCSD level, with an underestimation by 7.1%. These differences with respect to TMM originate from the γ_{yyyy} component of OXA that the UMPn methods strongly underestimate or even do not predict the correct (positive) sign. This is related to a wrong description of the strong field-induced charge-transfer effect along the CO bond (y axis). Subsequently, this wrong behavior cannot be corrected by the spin-projection schemes, except, to a given extent, with the UMP4 method where the value of -0.7 10^2 a.u. becomes 29 10^2 a.u. for *s*=4 but this is still 56.7% under the reference value. On the other hand, electron correlation effects on the γ_{xxxx} and γ_{zzzz} components present similar behaviors to those of TMM with differences between UMP4 (UMP2) and UCCSD(T) that attain 14 % (28 %). Again, the spin-projection effects are rather small but they improve the γ_{mean} estimates by about 3%.
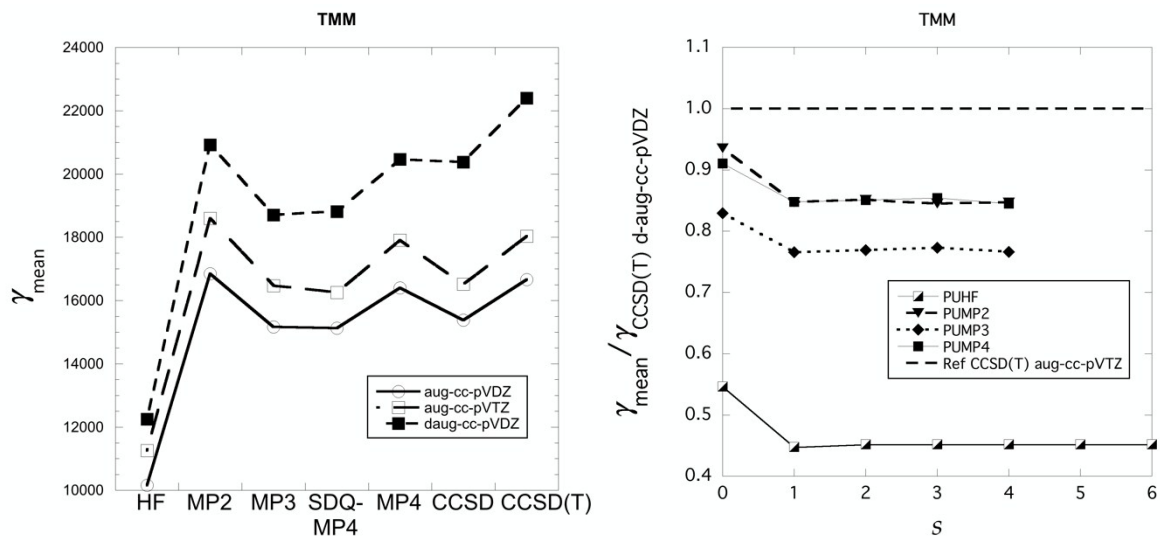
Figure 2. Basis set and electron correlation effects for wave function methods on the mean second hyperpolarizability of TMM. Lines are guides for the eyes. The left figure compares wave function correlated schemes to UCCSD(T) results for three basis sets whereas the right figure concentrates on spin-projected UHF, UMP2, UMP3, and UMP4 results obtained with the d-aug-cc-pvdz basis set.
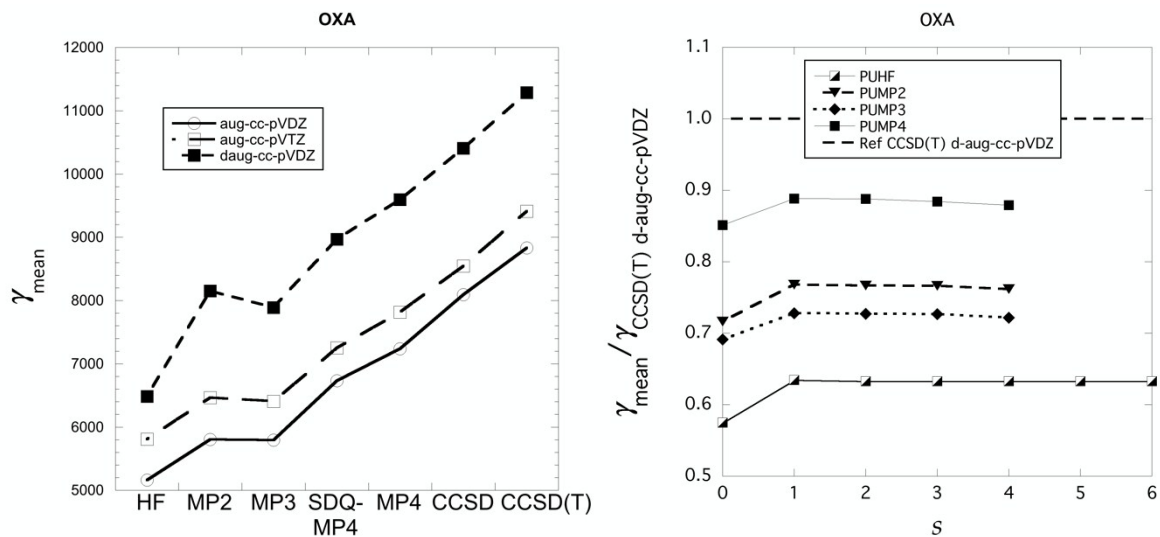
Figure 3. Basis set and electron correlation effects for wave function methods on the mean second hyperpolarizability of OXA. See Caption of Fig. 2 for more details.
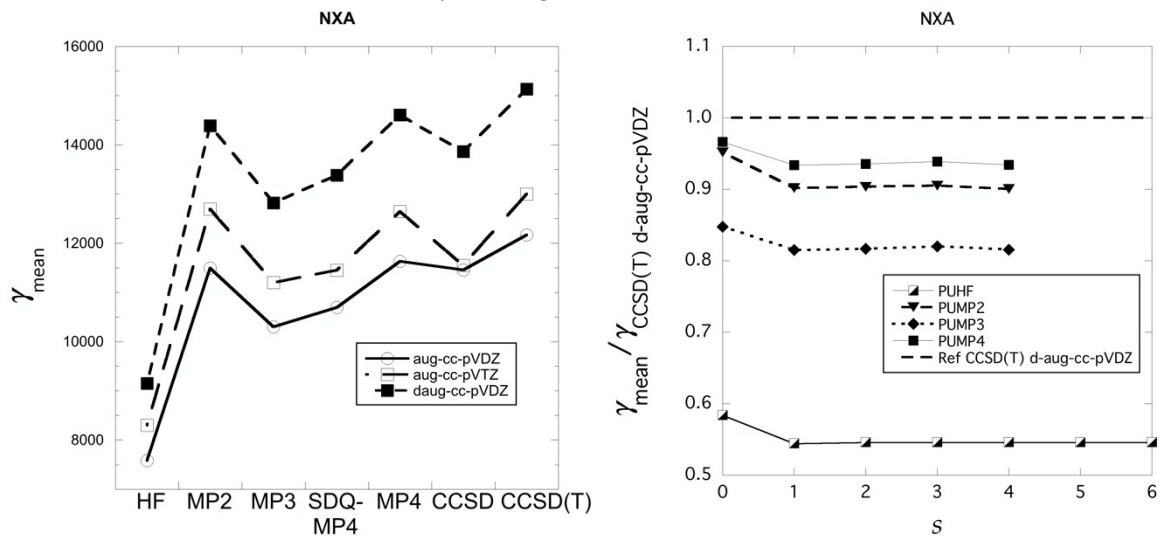
Figure 4. Basis set and electron correlation effects for wave function methods on the mean second hyperpolarizability of NXA. See Caption of Fig. 2 for more details.

γ_{mean}	TMM	OXA	NXA
UHF	122	65	91
UMP2	209	81	144
UMP3	187	79	128
SDQ-UMP4	188	90	134
UMP4	205	96	146
UCCSD	204	104	139
UCCSD(T)	**224**	**112**	**151**
P-UHF/s = 6	101	71	83
P-UMP2/s = 4	190	86	136
P-UMP3/s = 4	172	81	123
P-UMP4/s = 4	189	99	141

Table 1: d-aug-cc-pVDZ γ_{mean} values (in 10^2 a.u.) calculated at different levels of approximation.

For the NXA compound, the methods that best reproduce the UCCSD(T)/d-aug-cc-pVDZ value are UMP2 (-4.6%), UMP4 (-3.3%), and UCCSD (-7.9%), like for TMM. Since the charge-transfer contribution along the y-axis is weaker than for OXA, the UMPn methods do not present the same drawback for estimating γ_{yyyy}. Here also the spin-projection scheme is unable to improve the results; substantiating the usual weak spin contamination ($<S^2>$ = 2.19 at the UHF level of theory) of triplet states.

If we compare the UCCSD(T)/d-aug-cc-pVDZ values of the three compounds, the response of OXA is the weakest, followed by NXA and finally the strongest one is achieved for TMM. This can be explained in terms of structure/property relationships highlighting the role of the charge-transfer between the central and the doubly-bonded atom. Indeed, the response decreases with an increase of the charge transfer, which depends obviously on the electronegativity of the doubly-linked atom. The relationship between the charge-transfer and the electronegativity is substantiated by the UCCSD(T)/d-aug-cc-pVDZ dipole moment that amounts to 0.0, 1.1, and 0.8 a.u. for TMM, OXA, and NXA, respectively.

III.b. DENSITY FUNCTIONAL THEORY CALCULATIONS

In table 2 and figure 5, for the selected three basis sets, we compare DFT results obtained with different XC functionals to the reference UCCSD(T) values. For the three compounds, using the hybrid UB3LYP and UBHandHLYP functionals γ_{mean} systematically decreases with respect to the UBLYP functional, by about 30% for UB3LYP and 50% for UBhandHLYP. In the case of the LC-BLYP, a range-separating parameter of 0.33 appears more reliable to include the amount of HF exchange

needed to reproduce the UCCSD(T) reference values. For UM06 and UM06-2X, again the amount of HF exchange is important but only for the two compounds with charge-transfer (OXA and NXA).

Two XC functionals are able to reproduce quite well most of the reference computations. First, the LC-UBLYP functional with $\mu = 0.33$ reproduces well the UCCSD(T) values for OXA and NXA, with 1.8% and 4.0% of underestimation (d-aug-cc-pVDZ basis set). Unfortunately, for TMM the underestimation is larger (13.8%). Approximate spin-projected scheme does not change this conclusion. Then, the UM06-2X functional performs well for the three compounds, with overestimation of γ_{mean} of TMM by 4.5 %, a very good agreement for OXA, and a 1.3 % underestimation for NXA. Upon spin-projection, these values decrease by a few %, leading therefore to a better agreement for TMM but slightly worse for OXA and NXA. Note that the OXA molecule presents the smallest spin contamination among these compounds (see figure 5.d.).

γ_{mean}	TMM	OXA	NXA
UBLYP	352	213	260
UB3LYP	255	143	184
UBHandHLYP	183	96	130
LC-UBLYP $\mu = 0.33$	193	110	145
LC-UBLYP $\mu = 0.47$	151	83	111
UM06	234	131	190
UM06-2X	234	112	149
UCCSD(T)	**224**	**112**	**151**
P-UBLYP	332	205	250
P-UB3LYP	240	139	178
P-UBHandHLYP	174	94	126
P-LC-UBLYP $\mu = 0.33$	190	107	139
P-LC-UBLYP $\mu = 0.47$	151	82	107
P-UM06	219	126	163
P-UM06-2X	227	108	144

Table 2: d-aug-cc-pVDZ γ_{mean} values (in 10^2 a.u.) of TMM, OXA, and NXA as calculated with different XC functionals, in comparison to the reference UCCSD(T) values.
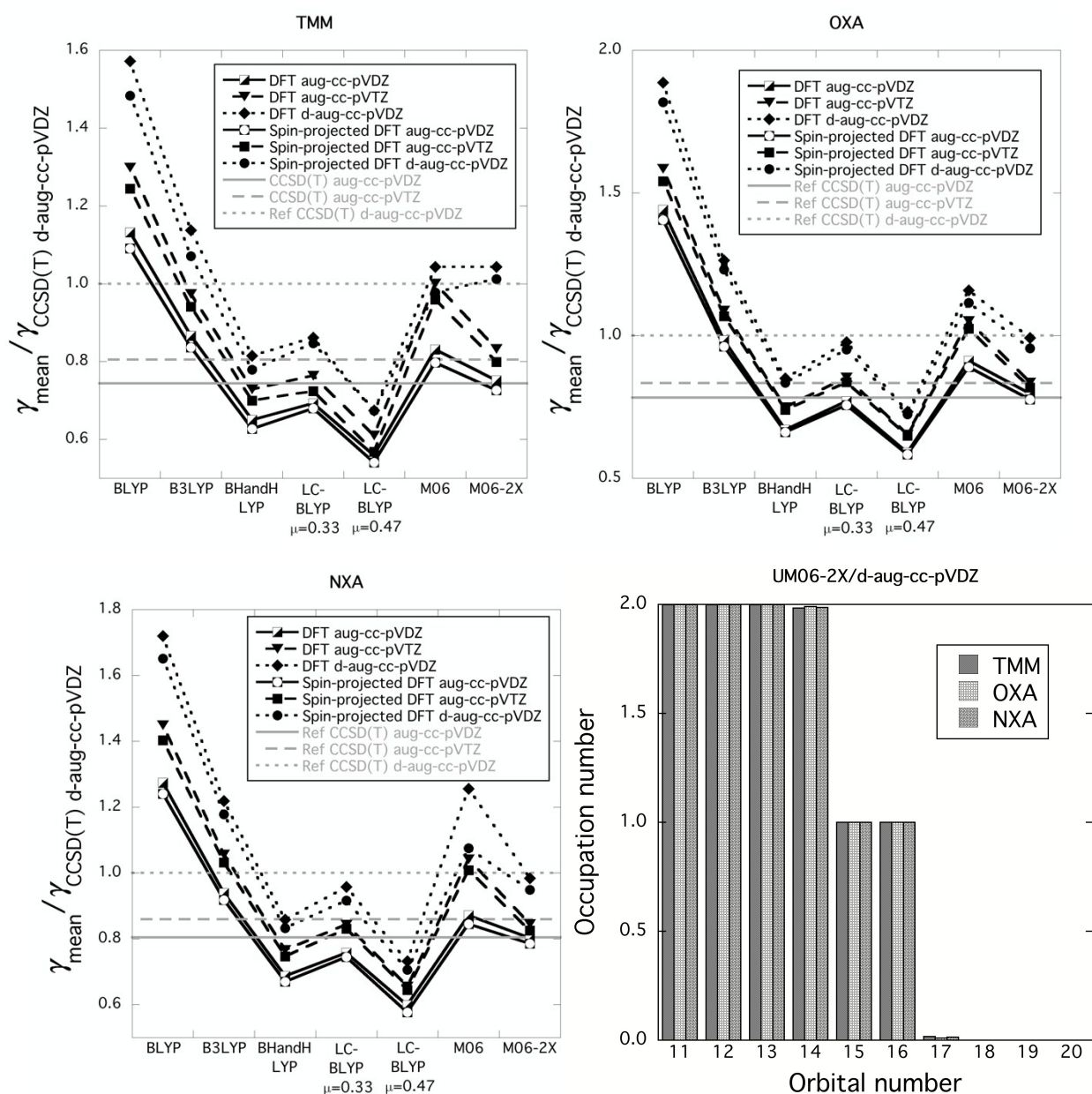
Figure 5. Basis set and electron correlation effects for DFT and approximate spin-projected DFT methods on the mean second hyperpolarizability of TMM, OXA, and NXA. Lines are guides for the eyes. The last figure shows the spin contamination as determined with UM06-2X XC functional.

To describe the spatial distribution of the open-shell character[91] the odd electron densities ($D^{odd}(\mathbf{r})$) are presented in figure 6. Those have been obtained as the summation of the odd electron densities of the 15th and 16th natural orbitals. In the case of TMM, the two radical electrons are localized almost equally on the three CH_2 moieties. For NXA, they are localized on the two CH_2 moieties but a little bit less on the NH group. Then, for OXA, the difference between the CH_2 moieties and the O atom is again slightly larger. Thus, in parallel to the increase of intramolecular charge-transfer (increase of the dipole moment), the amount of odd/diradical density on the "doubly-bonded" extremity (CH_2 for TMM, N for NXA, and O for OXA) decreases but it increases on the other sites. It must be noted that the odd electron density on the double-

11

bonded extremity results from contributions of both the 15th and 16th NOs. On the other hand, the contribution on each other extremity is mostly due to only one NO, NO 15th for one site and NO 16th for the other sites. In figure 6, the spin-projected UM06-2X/d-aug-cc-pVDZ γ densities employed to obtain the diagonal components of γ are also presented for the same isovalue of 15 a.u. These γ densities are converged, i.e. higher-order contaminations are removed by resorting to the Romberg procedure. Indeed, the integration of the position vector over the converged γ density tensor component grid leads to the same result as the Romberg procedure performed directly on the zeroth-order γ values obtained by relation (3). In the case of the γ_{xxxx} component, the γ density amplitude (and the tensor component) increases in parallel to 1°) the decrease of the odd electron density on the two CH_2 moieties and to 2°) the distance between these CH_2 moieties (2.52 Å for TMM, 2.49 Å for NXA, and 2.42 Å for OXA), highlighting the role of Pauli repulsion. For the γ_{yyyy} component, $d^{\gamma}_{yyy}(\vec{r})$ exhibits a decrease of its amplitude from TMM, to NXA, and to OXA. This is again associated to 1°) a reduction of the length of the double bond oriented along the y-axis (1.35, 1.28 and 1.20 Å, for TMM, NXA and OXA respectively), where the π-electrons are more localized, 2°) to the electronegativity of the heteroatom, and 3°) to the reduction of the odd electron density on the doubly-bonded atom. It noted that the 1°-3°) are related to each other since the heteroatom bond becomes stronger than the C=CH_2 bond due to the large difference of electronegativity (2°), which leads to shortening of the double-bond length (1°) and to reducing the odd electron density on the double bonded atoms (3°). For the γ_{zzzz} component, the response is proportional to $d^{\gamma}_{zzz}(\vec{r})$, which is larger for TMM, followed by NXA and then OXA, as shown in figure 6. It must be noted that for NXA, a part of the $d^{\gamma}_{zzz}(\vec{r})$ is hidden by the blue sphere representing the nitrogen atom. This explains why its contribution is larger than for OXA.

TMM	NXA	OXA

$D^{\text{odd}}(\mathbf{r})$

$\gamma^{SP}_{xxxx} = 204 \times 10^2 \, \text{a.u.}$ $\gamma^{SP}_{xxxx} = 176 \times 10^2 \, \text{a.u.}$ $\gamma^{SP}_{xxxx} = 152 \times 10^2 \, \text{a.u.}$

$\gamma^{SP}_{yyyy} = 199 \times 10^2 \, \text{a.u.}$ $\gamma^{SP}_{yyyy} = 98 \times 10^2 \, \text{a.u.}$ $\gamma^{SP}_{yyyy} = 65 \times 10^2 \, \text{a.u.}$

$\gamma^{SP}_{zzzz} = 177 \times 10^2 \, \text{a.u.}$ $\gamma^{SP}_{zzzz} = 114 \times 10^2 \, \text{a.u.}$ $\gamma^{SP}_{zzzz} = 108 \times 10^2 \, \text{a.u.}$
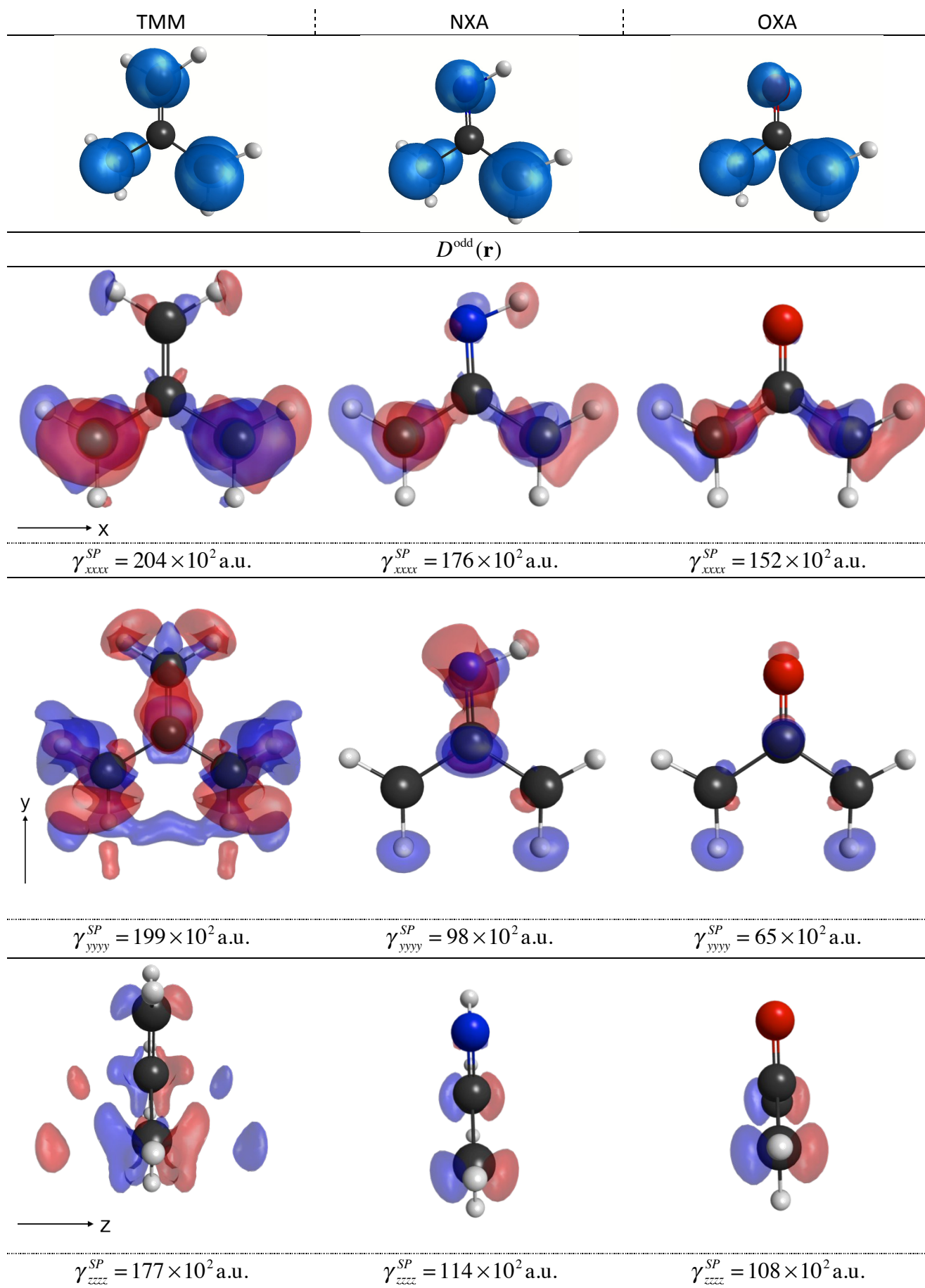
Figure 6. 1st row) Odd electron density (isovalue of 0.01 a.u.), 2nd-4th rows) spin-projected γ densities (isovalue of 15 a.u.) for each diagonal γ component as determined at the UM06-2X/d-aug-cc-pVDZ level (blue/red show positive/negative densities.

13

I.V. CONCLUSIONS

In this article, we have benchmarked a large set of methods with respect to UCCSD(T) for predicting the second hyperpolarizability (γ) of 1,3-dipole systems (TMM, NXA, and OXA) in their triplet state. These calculations have been performed with sufficiently extended atomic basis set and in particular with the d-aug-cc-pVDZ basis, which turns out to provide converged values. For the wave function methods, it appears that the UMP2, UMP4, and UCCSD methods can be used to characterize TMM and NXA but not OXA. In that case, the large field-induced charge transfer contribution is difficult to handle by the MPn methods and only the UCCSD method provides values close to the UCCSD(T) reference. It has also been shown that that the amplitude of the second hyperpolarizability response is strongly linked to the intramolecular charge-transfer, estimated by the permanent dipole moment: when the permanent dipole moment increases, the second hyperpolarizability decreases. Indeed, the presence of an heteroatom (X = N or O) is at the origin of 1°) an intramolecular charge transfer and therefore of a dipole moment, of 2°) a reduction of the C=X bond length, localizing the electrons and decreasing the γ component in that direction, and of 3°) an increase of the odd electron density on the CH_2 moieties, which enhances Pauli repulsion effects. Looking at DFT methods and at the performance of exchange-correlation functionals, the UM06-2X functional performs very well with a maximum of 4.5% of difference with respect to the UCCSD(T)/d-aug-cc-pVDZ reference values for these three compounds. This functional contains a substantial amount (54%) of HF exchange. Employing less HF exchange leads to an overestimation of the responses whereas range-separated hybrids underestimate to a given extent – that depends on the range-separating parameter – the second hyperpolarizabilities. The use of spin-projected methods for these 1,3-dipole triplet molecules has a little impact since the spin contamination is almost negligible, though for selected cases, it improves the results, including the the UM06-2X γ value of TMM.

Physical Chemistry Chemical Physics Accepted Manuscript

REFERENCES

1. H. Sekino and R. J. Bartlett, *J. Chem. Phys.*, 1993, **98**, 3022-3037.
2. M. Nakano, K. Yamaguchi, *Chem. Phys. Lett.,* 1993, **206**, 285-292.
3. M. Pecul, F. Pawlowski, P. Jorgensen, A. Köhn and C. Hättig, *J. Chem. Phys.*, 2006, **124**, 114101.
4. G. Maroulis, *J. Chem. Phys.*, 2008, **129**, 044314.
5. S.-L. Sun, G.-C. Yang, C.-S. Qin, Y.-Q. Qiu, L.-K. Yan, Z.-M. Su and R.-S. Wang, *Int. J. Quant. Chem.*, 2009, **110**, 865–873.
6. A. Baranowska and A. J. Sadlej, *J. Comput. Chem.*, 2010, **31**, 552-560.
7. M. Nakano, R. Kishi, T. Nitta, T. Kubo, K. Nakasuji, K. Kamada, K. Ohta, B. Champagne, E. Botek and K. Yamaguchi, *J. Phys. Chem. A*, 2005, **109**, 885-891.
8. P. C. Jha, Z. Rinkevicius and H. Ågren, *ChemPhysChem*, 2009, **10**, 817-823.
9. L. Serrano-Andres, A. Avramopoulos, J. Li, P. Labéguerie, D. Bégué, V. Kello and M. G. Papadopoulos, *J. Chem. Phys.*, 2009, **131**, 134312.
10. M. de Wergifosse, F. Wautelet, B. Champagne, R. Kishi, K. Fukuda, H. Matsui and M. Nakano, *J. Phys. Chem. A*, 2013.
11. M. Nakano, B. Champagne, *J. Phys. Chem. Lett.,* 2015, **6**, 3236-3256.
12. D.M. Bishop, B. Kirtman, H.A. Kurtz and J.E. Rice, *J. Chem. Phys.*, 1993, **98**, 8024.
13. A. Rizzo, S. Coriani, B. Fernandez and O. Christiansen, *Phys. Chem. Chem. Phys.*, 2002, **4**, 2884-2890.
14. J. R. Hammond and K. Kowalski, *J. Chem. Phys.*, 2009, **130**, 194108.
15. M. Hanauer and A. Kohn, *J. Chem. Phys.*, 2009, **131**, 124118.
16. H. L. Xu, F. F. Wang, Z. R. Li, B. Q. Wang, D. Wu, W. Chen, G. T. Yu, F. L. Gu and Y. Aoki, *J. Comput. Chem.*, 2009, **30**, 1128-1134.
17. P. A. Limacher, Q. Li and H. P. Luthi, *J. Chem. Phys.*, 2011, **135**, 014111.
18. S. Wouters, P.A. Limacher, D. Van Neck, and P.W. Ayers, *J. Chem. Phys.*, 2012, **136**, 134110.
19. M. Nakano, T. Minami, H. Fukui, R. Kishi, Y. Shigeta and B. Champagne, *J. Chem. Phys.*, 2012, **136**, 024315.
20. F. Castet, E. Bogdan, A. Plaquet, L. Ducasse, B. Champagne and V. Rodriguez, *J. Chem. Phys.*, 2012, **136**, 024506.
21. J. B. Robinson and P. J. Knowles, *J. Chem. Phys.*, 2012, **137**, 054301.
22. T. Yamada, Y. Inoue, B. Champagne and M. Nakano, *Chem. Phys. Lett.*, 2013, **579**, 73-77.
23. J.P. Coe and M.J. Paterson, *J. Chem. Phys.*, 2014, **141**, 124118.
24. M. de Wergifosse, F. Castet and B. Champagne, *J. Chem. Phys.,* 2015, **142**, 194102.
25. M. Kamiya, H. Sekino, T. Tsuneda and K. Hirao, *J. Chem. Phys.*, 2005, **122**, 234111.
26. R. Armiento, S. Kümmel and T. Körzdörfer, *Phys. Rev. B*, 2008, **77**, 165106.
27. C. D. Pemmaraju, S. Sanvito and K. Burke, *Phys. Rev. B*, 2008, **77**, 121204.
28. J. Messud, Z. Wang, P. M. Dinh, P. G. Reinhard and E. Suraud, *Chem. Phys. Lett.*, 2009, **479**, 300-305.
29. F. D. Vila, D. A. Strubbe, Y. Takimoto, X. Andrade, A. Rubio, S. G. Louie and J. J. Rehr, *J. Chem. Phys.*, 2010, **133**, 034111.

30. A. V. Arbuznikov and M. Kaupp, *Int. J. Quant. Chem.*, 2011, **111**, 2625-2638.
31. H. Fukui, Y. Inoue, R. Kishi, Y. Shigeta, B. Champagne and M. Nakano, *Chem. Phys. Lett.*, 2012, **523**, 60-64.
32. G. Maroulis, *Int. J. Quant. Chem.*, 2012, **112**, 2231-2241.
33. S. Nénon, B. Champagne and M. I. Spassova, *Phys. Chem. Chem. Phys.*, 2014, **16**, 7083-7088.
34. Y. Yokoi, H. Ishimaru, M. Kamiya and H. Sekino, *AIP Conf. Proc.*, 2015, **1649**, 135-140.
35. S. Yamada, M. Nakano, I. Shigemoto and K. Yamaguchi, *Chem. Phys. Lett.*, 1996, **254**, 158-161.
36. M. Nakano, H. Fujita, M. Takahata and K. Yamaguchi, *J. Am. Chem. Soc.*, 2002, **124**, 9648-9655.
37. M. Springborg, V. Tevekeliyska and B. Kirtman, *Phys. Rev. B*, 2010, **82**, 165442.
38. M. Nakano, S. Yamada and K. Yamaguchi, *Synth. Met.*, 1995, **71**, 1691-1692.
39. M. Nakano, I. Shigemoto, S. Yamada, K. Yamaguchi, *J. Chem. Phys.*, 1995, **103**, 4175-4191.
40. G. Maroulis, *J. Phys. Chem.*, 1996, **100**, 13466-13473.
41. G. Maroulis and C. Pouchan, *Phys. Rev. A*, 1998, **57**, 2440-2447.
42. S. Yamada, M. Nakano and K. Yamaguchi, *J. Phys. Chem. A*, 1999, **103**, 7105-7115.
43. D. Xenides and G. Maroulis, *Chem. Phys. Lett.*, 2000, **319**, 618-624.
44. M. Nakano, T. Nitta, K. Yamaguchi, B. Champagne and E. Botek, *J. Phys. Chem. A*, 2004, **108**, 4105-4111.
45. G. Maroulis and M. Menadakis, *Chem. Phys. Lett.*, 2010, **494**, 144.
46. P. Dowd, *J. Am. Chem. Soc.*, 1966, **88**, 2587-2589.
47. R. J. Baseman, D. W. Pratt, M. Chow and P. Dowd, *J. Am. Chem. Soc.*, 1976, **98**, 5726-5727.
48. P. Dowd and M. Chow, *Tetrahedron*, 1982, **38**, 799-807.
49. P. Dowd and M. Chow, *J. Am. Chem. Soc.*, 1977, **99**, 6438-6440.
50. P. G. Wenthold, J. Hu, R. R. Squires and W. C. Lineberger, *J. Am. Chem. Soc.*, 1996, **118**, 475-476.
51. F. Weiss, *Quart. Rev., Chem. Soc.*, 1970, **24**, 278-309.
52. P. Dowd, *Accounts Chem. Res.*, 1972, **5**, 242-248.
53. D. R. Yarkony and H. F. Schaefer, III, *J. Am. Chem. Soc.*, 1974, **96**, 3754-3758.
54. W. J. Hehre, L. Salem and M. R. Willcott, *J. Am. Chem. Soc.*, 1974, **96**, 4328-4330.
55. J. H. Davis and W. A. Goddard, III, *J. Am. Chem. Soc.*, 1977, **99**, 4242-4247.
56. W. T. Borden and E. R. Davidson, *J. Am. Chem. Soc.*, 1977, **99**, 4587-4594.
57. E. R. Davidson and W. T. Borden, *J. Am. Chem. Soc.*, 1977, **99**, 2053-2060.
58. J. A. Berson, *Acc. Chem. Res.*, 1978, **11**, 446-453.
59. A. A. Ovchinnikov, *Theor. Chim. Acta*, 1978, **47**, 297-304.
60. D. A. Dixon, R. Foster, T. A. Halgren and W. N. Lipscomb, *J. Am. Chem. Soc.*, 1978, **100**, 1359-1365.
61. D. M. Hood, R. M. Pitzer and H. F. Schaefer, III, *J. Am. Chem. Soc.*, 1978, **100**, 2227-2228.
62. D. M. Hood, H. F. Schaefer, III and R. M. Pitzer, *J. Am. Chem. Soc.*, 1978, **100**, 8009.
63. W. T. Borden and E. R. Davidson, *Acc. Chem. Res.*, 1981, **14**, 69-76.
64. D. Feller, W. T. Borden and E. R. Davidson, *J. Chem. Phys.*, 1981, **74**, 2256-2259.
65. D. Feller, K. Tanaka, E. R. Davidson and W. T. Borden, *J. Am. Chem. Soc.*, 1982, **104**, 967-972.
66. S. B. Auster, R. M. Pitzer and M. S. Platz, *J. Am. Chem. Soc.*, 1982, **104**, 3812-3815.
67. W. T. Borden, E. R. Davidson and D. Feller, *Tetrahedron*, 1982, **38**, 737-739.
68. P. M. Lahti, A. Rossi and J. A. Berson, *J. Am. Chem. Soc.*, 1985, **107**, 2273-2280.
69. S. Olivella and J. Salvador, *Int. J. Quantum Chem.*, 1990, **37**, 713-728.
70. C. P. Blahous, III, Y. Xie and H. F. Schaefer, III, *J. Chem. Phys.*, 1990, **92**, 1174-1179.
71. T. P. Radhakrishnan, *Tetrahedron Lett.*, 1991, **32**, 4601-4602.
72. W. T. Borden, H. Iwamura and J. A. Berson, *Acc. Chem. Res.*, 1994, **27**, 109-116.
73. A. S. Ichimura, N. Koga and H. Iwamura, *J. Phys. Org. Chem.*, 1994, **7**, 207-217.
74. W. T. Borden, *Mol. Cryst. Liq. Cryst. Sci. Technol., Sect. A*, 1993, **232**, 195-218.

75. C. J. Cramer and B. A. Smith, *J. Phys. Chem.*, 1996, **100**, 9664-9670.
76. B. Ma and H. F. Schaefer, III, *Chem. Phys.*, 1996, **207**, 31-41.
77. A. Lewis, A. Khatchatouriants, M. Treinin, Z. Chen, G. Peleg, N. Friedman, O. Bouevitch, Z. Rothman, L. Loew and M. Sheres, *Chem. Phys.*, 1999, **245**, 133-144.
78. L. V. Slipchenko and A. I. Krylov, *J. Chem. Phys.*, 2003, **118**, 6874-6883.
79. A. Dworkin, R. Naumann, C. Seigfred, J. M. Karty and Y. Mo, *J. Org. Chem.*, 2005, **70**, 7605-7616.
80. D. Casanova, L. V. Slipchenko, A. I. Krylov and M. Head-Gordon, *J. Chem. Phys.*, 2009, **130**, 044103.
81. X. Lopez, F. Ruipérez, M. Piris, J. M. Matxain and J. M. Ugalde, *ChemPhysChem*, 2011, **12**, 1061-1065.
82. J. Shen and P. Piecuch, *J. Chem. Phys.*, 2013, **138**, 194102.
83. M. Nakano, T. Minami, H. Fukui, R. Kishi, Y. Shigeta and B. Champagne, *J. Chem. Phys.*, 2012, **136**, 024315.
84. B. Champagne, E. Botek, O. Quinet, M. Nakano, R. Kishi, T. Nitta and K. Yamaguchi, *Chem. Phys. Lett.*, 2005, **407**, 372-378.
85. R. Kishi, S. Bonness, K. Yoneda, H. Takahashi, M. Nakano, E. Botek, B. Champagne, T. Kubo, K. Kamada, K. Ohta and T. Tsuneda, *J. Chem. Phys.*, 2010, **132**, 094107.
86. M. de Wergifosse, V. Liégeois and B. Champagne, *Int. J. Quant. Chem.*, 2014, **114**, 900-910.
87. M. J. Frisch, G. W. Trucks, H. B. Schlegel, G. E. Scuseria, M. A. Robb, J. R. Cheeseman, G. Scalmani, V. Barone, B. Mennucci, G. A. Petersson, H. Nakatsuji, M. Caricato, X. Li, H. P. Hratchian, A. F. Izmaylov, J. Bloino, G. Zheng, J. L. Sonnenberg, M. Hada, M. Ehara, K. Toyota, R. Fukuda, J. Hasegawa, M. Ishida, T. Nakajima, Y. Honda, O. Kitao, H. Nakai, T. Vreven, J. A. Montgomery, J. E. Peralta, F. Ogliaro, M. Bearpark, J. J. Heyd, E. Brothers, K. N. Kudin, V. N. Staroverov, R. Kobayashi, J. Normand, K. Raghavachari, A. Rendell, J. C. Burant, S. S. Iyengar, J. Tomasi, M. Cossi, N. Rega, J. M. Millam, M. Klene, J. E. Knox, J. B. Cross, V. Bakken, C. Adamo, J. Jaramillo, R. Gomperts, R. E. Stratmann, O. Yazyev, A. J. Austin, R. Cammi, C. Pomelli, J. W. Ochterski, R. L. Martin, K. Morokuma, V. G. Zakrzewski, G. A. Voth, P. Salvador, J. J. Dannenberg, S. Dapprich, A. D. Daniels, Farkas, J. B. Foresman, J. V. Ortiz, J. Cioslowski and D. J. Fox, Wallingford CT2009.
88. P.-O. Löwdin, *Phys. Rev.*, 1955, **97**, 1509-1520.
89. S. Bonness, H. Fukui, K. Yoneda, R. Kishi, B. Champagne, E. Botek and M. Nakano, *Chem. Phys. Lett.*, 2010, **493**, 195-199.
90. M. Nakano, H. Fukui, T. Minami, K. Yoneda, Y. Shigeta, R. Kishi, B. Champagne, E. Botek, T. Kubo, K. Ohta and K. Kamada, *Theor Chem Acc*, 2011, **130**, 711-724; *erratum* **130**, 725.
91. K. Yoneda, M. Nakano, K. Fukuda and B. Champagne, *J. Phys. Chem. Lett.*, 2012, **3**, 3338-3342.